CGU HS Committee on River Ice Processes and the Environment
14th Workshop on the Hydraulics of Ice Covered Rivers
Quebec City, June 19 - 22, 2007

River Ice Breakup Strength Criteria

Nzokou T.F[1], Morse B.[2], Roubtsova V.[3], Quach T.[4]
[1]*Université Laval, Québec, QC, Canada, E-mail: Francois.Nzokou.1@ulaval.ca*
[2]*Université Laval, Québec, QC, Canada, E-mail: Brian.Morse@gci.ulaval.ca*
[3]*École Polytechnique de Montréal, Montréal, QC, Canada, varvara.roubtsova@gmail.com*
[4] *Hydro-Québec, Montréal, Québec, Canada. E-mail: Quach_Thanh.Tung@hydro.qc.ca*

It has been shown that the propagation of a breakup surge in impeded rivers differs from the unimpeded case. The ice cover affects both the wave celerity and magnitude, but this effect can't be evaluated efficiently without a thorough investigation of the water wave and intact ice cover interaction. In other words we need to know what flow and water level variations an ice cover can withstand, on a specific river reach, before rupturing. Once the ice fails it is also important to evaluate how the wave characteristics are changed. In the frame of this study a theoretical analysis of the water and ice interaction is carried out. Both 1D and 2D approaches are used. The 1D approach is based on the theory of beams on elastic foundations, and aims to formulate a simple criteria that can be incorporated to 1D hydraulic models. The 2D approach is based on the theory of plates on elastic foundation and aims to evaluate the effect of the banks resistance and constraint on the shape of the cracks and on the ice cover overall resistance. A parametric analysis is also carried out to evaluate the effect of the water wave; river and ice cover characteristics on the proposed breaking criteria. The parametric study also attempts to guide the field investigation by outlining the most important parameters for the phenomenon. The strength and limitations of the 1D approach are outlined.

1. Context

The water wave and ice cover interaction has been studied by numerous scientists in the past. Xia and Shen (2002) carried out a non linear analysis on the interaction of shallow water wave with a freely floating ice cover in a uniform channel. The authors then derived a weakly non-linear wave equation with dispersion terms due to ice bending, ice inertia and axial forces on the ice. Xia and Shen found that a) the presence of ice slightly reduces the wave speed; b) the minimum wave height required to fracture the ice cover is typically in the range of 0.2 to 0.8 m, depending on the cover thickness and strength. The corresponding wavelength varies between 50 and 400 m. According to the authors the transverse crack spacing corresponds to the wavelength. Assuming sinusoidal water and flexural waves propagating in phase under and within an infinitely long ice cover, Daly (1993, 1995) linearized the equations of motion and determined the wave celerity as a function of channel characteristics and ice properties. His study was further refined in a discussion by Steffler and Hicks (1994). Considering a wave of linear shape, Billfalk (1982) showed that the maximum bending moment occurs at the nose of the wave. This result was further confirmed by Beltaos (2004) who considered sinusoidal waves. Beltaos further showed that for long waves, the wave needed to advance by just the quarter of its length into the ice cover to induce the maximum stress on the ice. In this range, stress showed to be a direct proportion of the average wave slope expressed by the quantity (w_0/ (L/4))

$$S_w = \frac{w_0}{\left(L/4\right)} \equiv K \frac{l}{h} \frac{\sigma}{E} \qquad \textbf{[1]}$$

Where w_0 and L are the wave amplitude and length respectively; h is the ice thickness; l the characteristic length of the ice; E Young's modulus; and K is a numerical parameter having the value 4. One difficulty in applying this relation lies in the estimation of the wave length. Moreover, the effect of the wave amplitude can not be evaluated directly since it is incorporated in the term S_w. In fact, a wave with a given length might have different amplitudes and as a result induce various loading scenarios when it comes in contact of an ice cover. Considering a linear wave approximation, Billfalk (1982) found a relation to the stress in the ice sheet which can be seen as a function of the increase in river slope:

$$\frac{\Delta H_{\max}}{l} \geq \frac{1}{3.28} \frac{1}{h^{\frac{1}{4}}} \frac{\sigma}{E^{\frac{3}{4}}} \qquad \textbf{[2]}$$

where ΔH_{max} is the wave height (equivalent to wave amplitude)

2. Objectives

This study aims to continue these investigations in order to derive a simple breaking criteria that can be implemented to 1D numerical model applications of river breakup. From the conclusions of above analyses, it is obvious that this criterion should be a direct function of the rate of water

level increase as well as the amplitude of this increase. The initial analysis will, as in previous studies, be based on the 1D theory of beam on elastic foundation presented by Hetenyi (1946). In addition, a 2D analysis will also be carried out in order to investigate the banks effects and improve the conclusions of a 1D approach. The 2D analysis will be based on the theory of plates on elastic foundation presented by Timoshenko (1959).

3. 1-D analysis

3.1. Introduction

The differential equation for the deflection curve of a beam supported on an elastic foundation is given by Hetenyi (1946). If, as shown on Figure 1, a single concentrated load P is applied at a certain distance "*a*" from the free edge of the beam the differential equation will be:

$$EI\frac{d^4y}{dx^4} = -ky + P \qquad \textbf{[3]}$$

In this equation y is the deflexion of the beam; I, the moment of inertia per unit width ($I=h^3/12$); and k the foundation modulus. Hetenyi showed that the solution to equation [3] can be expressed as:

$$\begin{cases} y(x) = \dfrac{P\lambda}{2k}\left[\left(C_{\lambda a} + 2D_{\lambda a}\right)A_{\lambda x} - 2\left(C_{\lambda a} + D_{\lambda a}\right)B_{\lambda x} + A_{\lambda\lfloor a-x\rfloor}\right] \\ M(x) = \dfrac{P}{4\lambda}\left[\left(C_{\lambda a} + 2D_{\lambda a}\right)C_{\lambda x} - 2\left(C_{\lambda a} + D_{\lambda a}\right)D_{\lambda x} + C_{\lambda\lfloor a-x\rfloor}\right] \end{cases} \qquad \textbf{[4]}$$

with

$$\begin{cases} A_{\lambda x} = e^{-\lambda x}\left(\cos\lambda x + \sin\lambda x\right) \\ B_{\lambda x} = e^{-\lambda x}\sin\lambda x \\ C_{\lambda x} = e^{-\lambda x}\left(\cos\lambda x - \sin\lambda x\right) \\ D_{\lambda x} = e^{-\lambda x}\cos\lambda x \end{cases} \qquad \textbf{[5]}$$

M is the bending moment and λ is a parameter given by:

$$\lambda = \left(\frac{\gamma}{4EI}\right)^{\frac{1}{4}} \qquad \textbf{[6]}$$

where γ is the unit weight of water. The term $1/\lambda$ having the dimension of a length, was referred to as the characteristic length by Hetenyi. Other authors gave the following relationship to define the characteristic length (e.g Ashton, 1986; Beltaos, 1993):

$$l = \left(\frac{Eh^3}{12\gamma\left(1-\nu^2\right)} \right)^{\frac{1}{4}} \qquad [7]$$

where v is the Poisson's ratio (≈ 0.33).

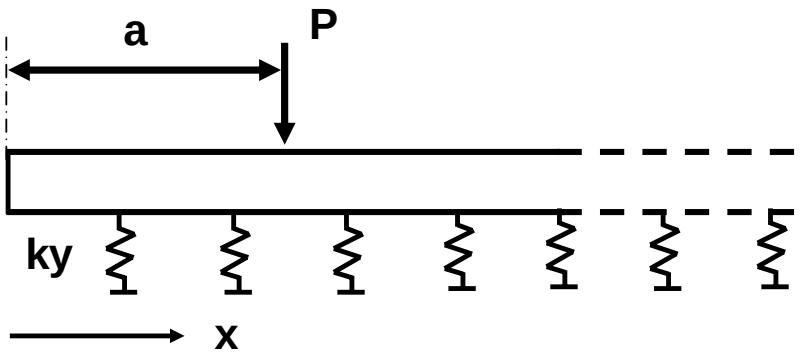

Figure 1 : Semi-infinite beam resting on a elastic foundation subjected to a single load applied at a distance a from the free edge

3.2. Method of superposition

Figure 2, depicts the method by which a triangular wave is approximated by a series of n point loads applied at the center of each cell. The smaller the cell size Δx, the more precise will be the approximation.

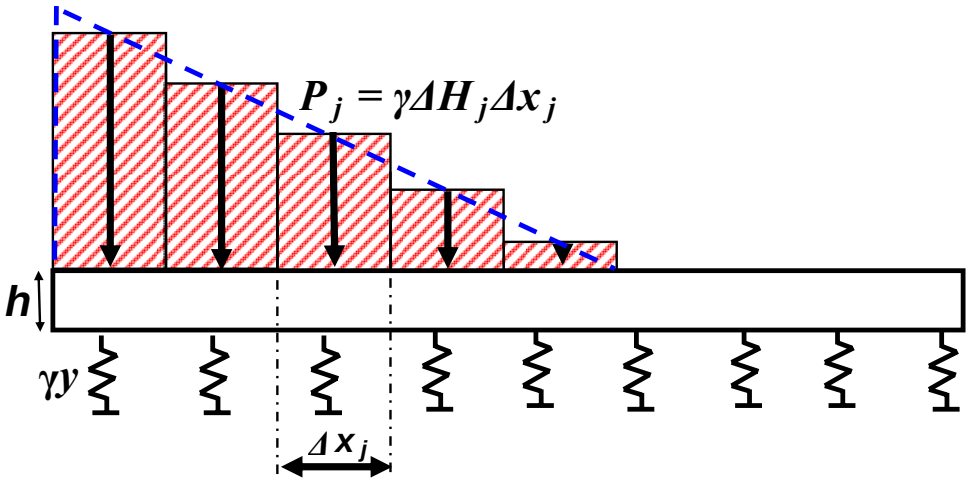

Figure 2 : Approximation of a triangular wave with point loads applied at the center of each cell

The load at each division 'j' of the domain is given by :

$$P_j = -\gamma \Delta H_j \Delta x_j \qquad \text{with} \qquad j = 1..n \qquad [8]$$

For each load P_j, the deflection y_j and bending moment M_j are computed using equation [4]. By superposition of the individual solutions, the complete solution is obtained,

$$\begin{cases} y = \sum_{j=1}^{n} y_j \\ M = \sum_{j=1}^{n} M_j \end{cases} \qquad [9]$$

3.3. Adaptation of Hetenyi's solution to the bending of floating ice cover

The solution to equation [3] is obtained iteratively. Figure 3 shows a situation where an incoming water wave of 1m height has advanced by 100 m into a 1 m thick and 200 m long ice cover. Plotted here are the ice and water profiles after the solution has converged. The vertical scale is exaggerated to make easier to see. In Figure 3a, the static load applied on the cover is computer using equation [8] with no limitation imposed on p_r. This is not the case when looking at the behavior of an ice cover floating at the surface of water. The difference between these two plots resulting in the bounds that should be imposed on p_r are explained next.

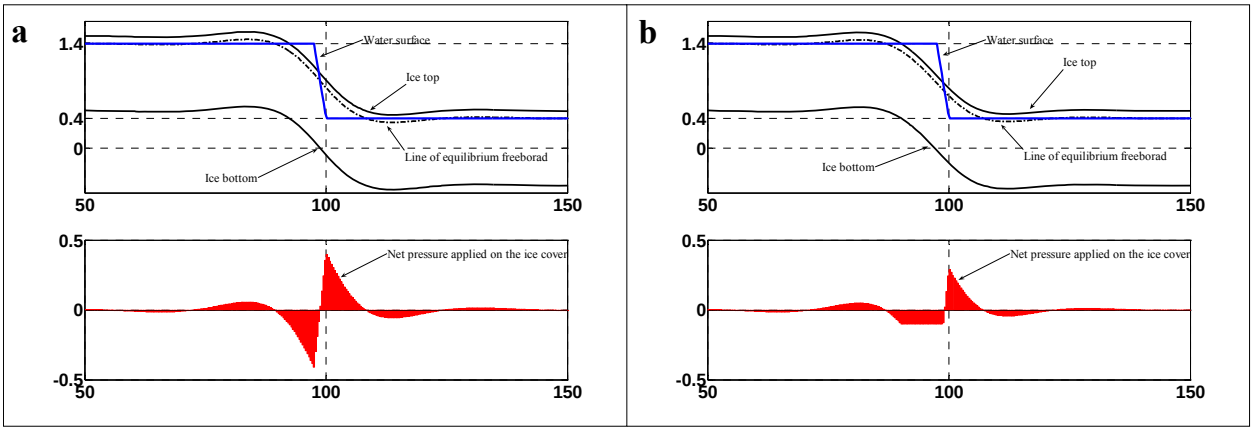

Figure 3 : Net pressure on floating ice cover subjected to incoming water wave a) Mathematical application of Hetenyis solution b) Real solution taking into account floating ice specificities

Generally, when the ice cover is at equilibrium at the surface of the water, there is no load applied on it. The submerged part of the ice cover h_s is given by $s_i h$ with h being the ice thickness and s_i the ratio of the ice to water density. Naturally, the equilibrium freeboard is given by $(1-s_i)h$. As soon as the ice and/or the water level changes, a reaction load is then created trying to bring the system back into equilibrium. The magnitude and direction of this reaction load depends on the position of ice cover compare to water surface. If the freeboard is less than the equilibrium freeboard $(1-s_i)h$, an uplift pressure is generated. This uplift pressure is proportional to difference between the water level change and the ice deflection $(y-\Delta H)$. As soon as the ice cover is completely submerged, the uplift pressure reaches a maximum value of $\gamma(1-s_i)h$ which is independent of the degree of submergence of the ice cover. If instead the freeboard increases and get greater than $(1-s_i)h$, the weight of the afloat part of the ice exceeds the buoyancy force. This results in a downward pressure which is again proportional to the difference $(y-\Delta H)$. The downward pressure can not exceed a value of $\gamma s_i h$ which corresponds to the situation where the ice cover is completely out of water. In general, considering the positive direction downward, the net pressure is be bounded by:

$$-(1-s_i)h \le p_r = \gamma(y-\Delta H) \le s_i h \qquad \textbf{[10]}$$

Equation [10] holds regardless of whether the ice cover is submerged or not. For a 1 m thick ice having a density of 900 kg/m³, p_r is between -0.1 and 0.9 N/m²/m. In Figure 3a, the load is computed without any limitation and as expected, the minimum net pressure (-0.4/m²/m) is out of the above physical bound. When taking equation [10] into account, the load at each division '*j*' of the domain is now given by:

$$P_j = -\gamma \Delta H_j \Delta x_j \qquad \text{with} \qquad j = 1..n \quad ; \quad -y_j - s_i h \le \Delta H_j \le -y_j + (1-s_i)h \qquad \textbf{[11]}$$

The resulting loading profile shown on Figure 3b now has a physical meaning.
The above result suggests that two things need to be considered when applying Hetenyi's solution (equation [4]) to solve bending of an ice cover floating on the water surface. First, the solution method must be iterative to make sure the stresses fully develop in the ice cover. Secondly, the net pressure applied at each iteration step must be bounded as shown by equation [10].

3.4. Ice response to various wave front

Equation [4] together with condition [10] will be applied to analyze the bending of a semi-infinite ice cover, freely floating at the surface of water. Various wave shapes will be considered. First a sinusoidal long wave (kl = 0.25) that has advanced by a quarter of its length into the ice cover; then a linear triangular waves with various water surface slopes. Figure 4a depicts the different wave profiles. The ice response to these waves is presented in Figure 4b the induced flexural stresses in Figure 4c. On these figures the ice responses, the waves and the flexural stresses are expressed in their dimensionless forms; respectively as:

$$y_d = \frac{y}{\Delta H_{\max}} \qquad \textbf{[12]}$$

$$\Delta H_d = \frac{\Delta H}{\Delta H_{\max}} \qquad \textbf{[13]}$$

and

$$\sigma_d = \frac{l^2}{h \Delta H_{\max}} \frac{\sigma}{E} \qquad \textbf{[14]}$$

σ is the flexural stress computed from the bending moment M ($\sigma = \frac{6M}{h^2}$).

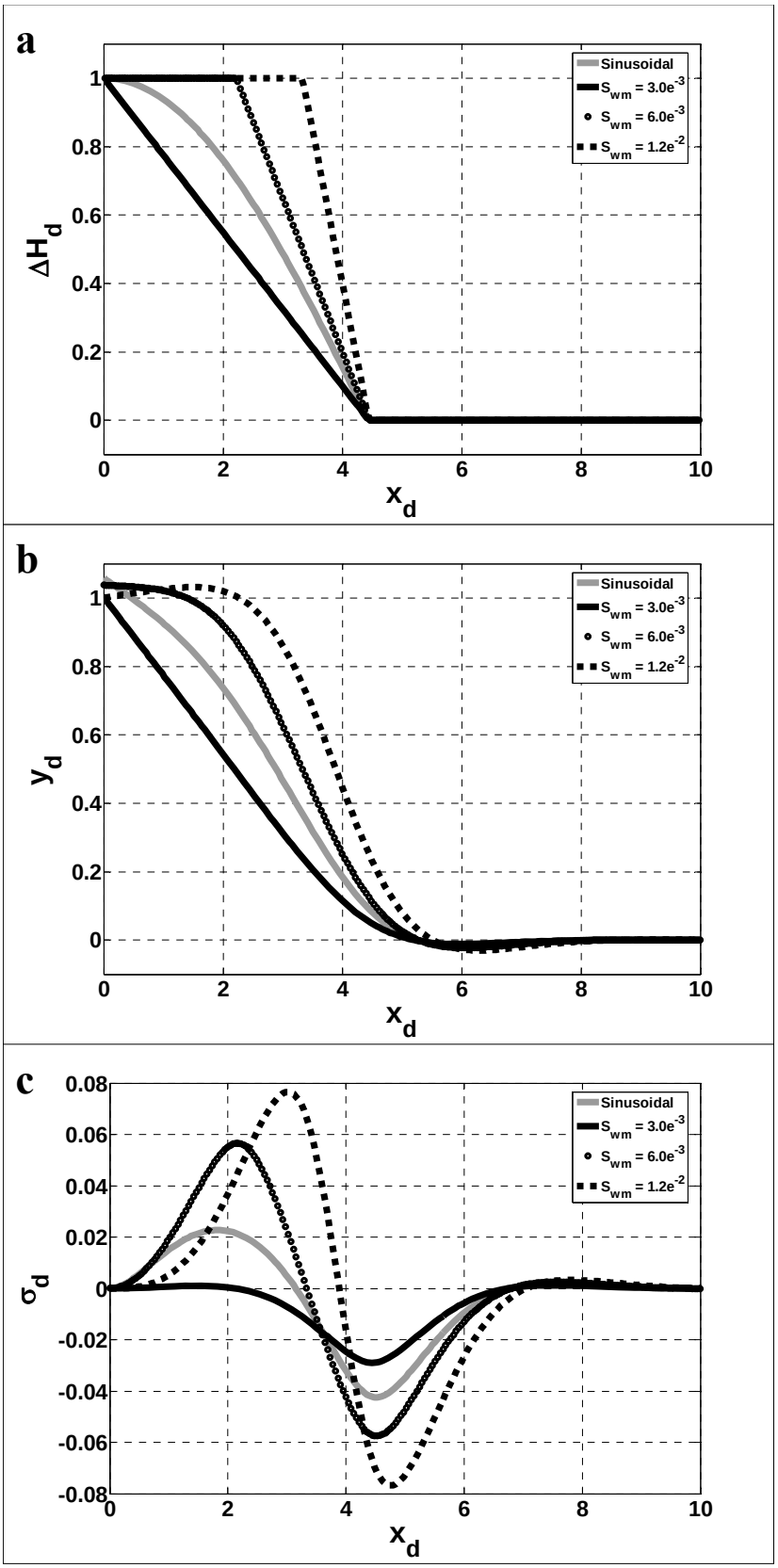

Figure 4 : Ice cover response (b) and induced stress in the ice cover (c) due to various wave fronts (a).

Regardless of the front shape, the maximum stress develops close to the wave front as soon as the wave reaches it amplitude (ΔH_{max}) and stays unchanged for further advancement. Billfalk (1982) and Beltaos (2004) found similar results. Secondly, at equal amplitudes, the induced stress increases with the mean water surface slope. Thirdly, additional tests for other amplitudes show that, at equal front slope, the induce stress increases with the increasing wave amplitude. The change in water level given by (ΔH_{max}) and the rate of change in water level, given indirectly by the front slope (S_w) are both determining parameters in inducing peak stresses in the ice cover. The effect of each parameter will be presented in the two sub-sections that follow.

3.5. Effect of the front slope on the peak stress induced

The model is run for linear wave with front slopes (S_w) varying between 5.10^{-4} and 8.10^{-3}. The resulting stress was examined and the maximum of peak values (in absolute terms either positive or negative) was noted σ_{dmax} and are plotted on Figure 5. Ice thicknesses ranging between h = 0.2 and 3 m were considered. This represents a larger range than what is usually observed in nature.

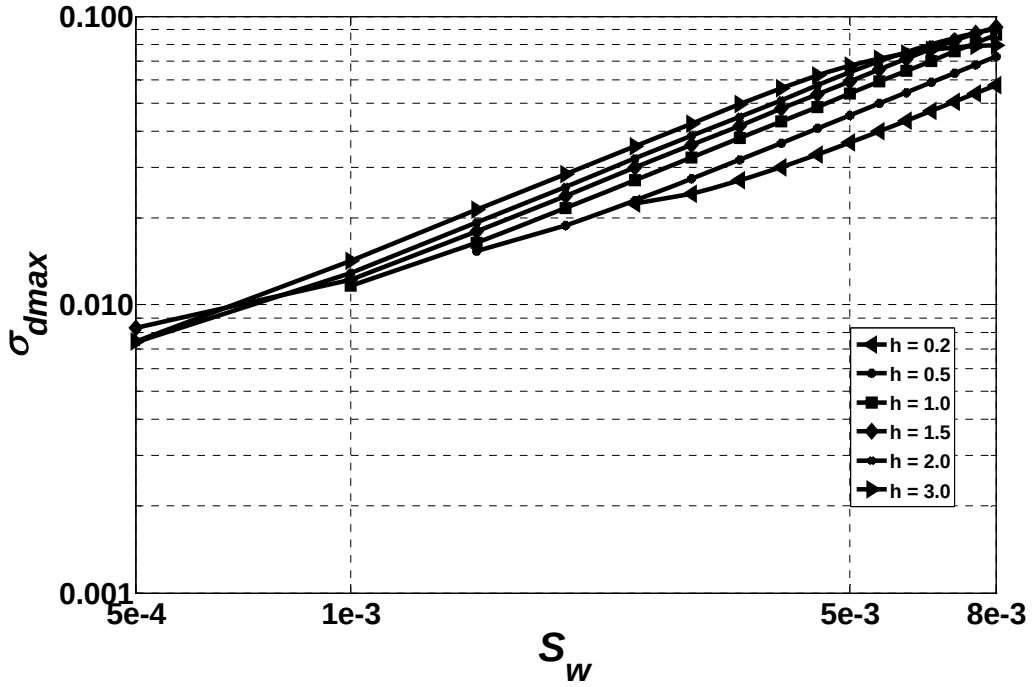

Figure 5 : Variation of peak dimensionless stress as a function of the mean front slope (S_w).

Looking at the above plots, over a large range of S_w, the peak stress can reasonably be approximated by linear function of S_w,

$$\sigma_{d\max} = K_1 S_w \qquad \textbf{[15]}$$

With K_1 being an empirical coefficient having a value approximately equal to 10. Equations [14] and [15] can be combined, rearranged to obtain an expression for the water surface slope S_w:

$$S_w \equiv K_2 \frac{l^2}{h\Delta H_{\max}} \frac{\sigma}{E} \qquad \textbf{[16]}$$

Where K_2 is a numerical coefficient $K_2 = 1/K_1 \approx 0.10$. Using equation [16], the average water surface slope required to fracture an ice cover can be evaluated. For example, if the ice cover is 0.5 m thick, has a maximum critical flexural stress of $\sigma_c = 0.5$ MPa and a Young's modulus of $E = 9$ GPa, equation [16] will yield a critical increase of surface slope of $S_w = 4 \times 10^{-3}$. Increase in water slope values in this range have been reported for field conditions and have been predicted by previous theoretical investigations. For example, during dynamic ice jam release on the Athabasca River, (Kowalczyk et al., 2003), wave and attenuation data was successfully documented over a 40 km reach. Rough estimate of the average increase of water surface slope on the graphs in the above mentioned publication gave values in the range of 3.10^{-3}. The ice cover characteristics were not given. Xia and Shen (2002) carried out a non linear analysis on the water wave and ice cover interaction and found that to break an ice cover having a thickness of 1 m, a Young modulus 10 GPa and a flexural strength of 0.6MPa, a cnoidal water wave of 0.3 m amplitude and a length of 382 m was required. An estimated of the front slope of this wave gives approximately 3.10^{-3}.

Figure 6 shows the profiles of the increase in mean water slopes computed with equations [1], [2] and [16] respectively from Beltaos (2004), Billfalk (1982) and from the present analysis. In all cases the ice resistance ranges from 0.5 to 1.2 MPa, the ice thickness is 1 m, $E = 9$ GPa, the wave height is 0.5m.

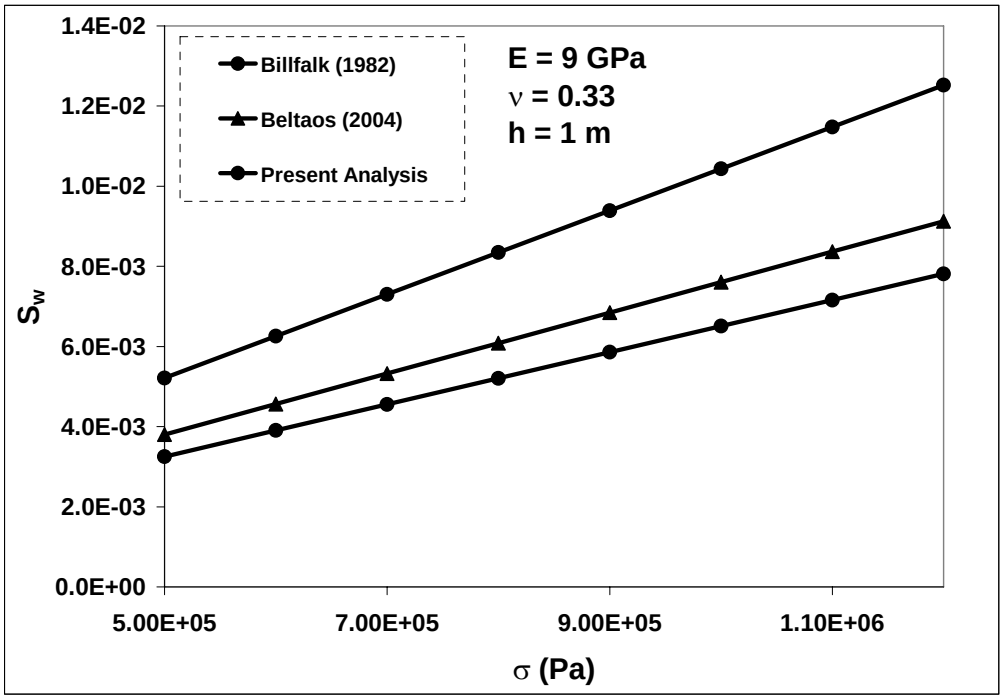

Figure 6 : Mean water slope as a function of the ice resistance. Results from previous and present analysis

The figure above shows that, for given ice and water wave properties, the mean critical slopes from the three equations are comparable. The main difference lies in the presence of the wave height (ΔH_{max}) at the denominator of equation [16] from the actual analysis. The effect of this wave amplitude will be presented later in section 3.7.

3.6. Sensitivity of the front slope criteria to the ice mechanical properties

3.6.1. Flexural Strength

A summary of a number of measurements of ice flexural strength carried out by various authors is presented by Ashton (1986). From these measurements, the expected bending strength of competent, columnar freshwater ice ranges from a low of 0.5 MPa for relatively large specimens tested by the cantilever beam method to a high of 1.2 MPa for small, simple beam specimens. This range of values also reflects differences in results obtained depending on whether the tests were conducted with the top of the ice under tension or the bottom of the ice under tension and the corresponding variation in crystal size. Strength apparently decreases with increasing sample size and is also influenced by strain rate and type of test. Flexural strength is little affected by temperature, except when the ice cover actually begins to deteriorate (USACE, 1999 and Butyagin, 1972). The main cause of this deterioration is internal melt, occurring at crystal boundaries, known sites of concentration of foreign occlusions. The presence of foreign matter or impurities lowers the melting point, which causes preferential melt as soon as the internal temperature of the ice approaches 0°C.

To investigate the sensitivity of the breaking criteria to the flexural strength, the flexural strength was varied between 0.5 MPa and 1.2 MPa as suggested by measurements reported previously. Ice cover thicknesses ranging from 0.2 to 2 m where used. The elastic modulus was set to 9GPa and the Poisson's ratio to 0.33. Figure 7 depicts the variation of the critical water surface slope as a function of the flexural strength

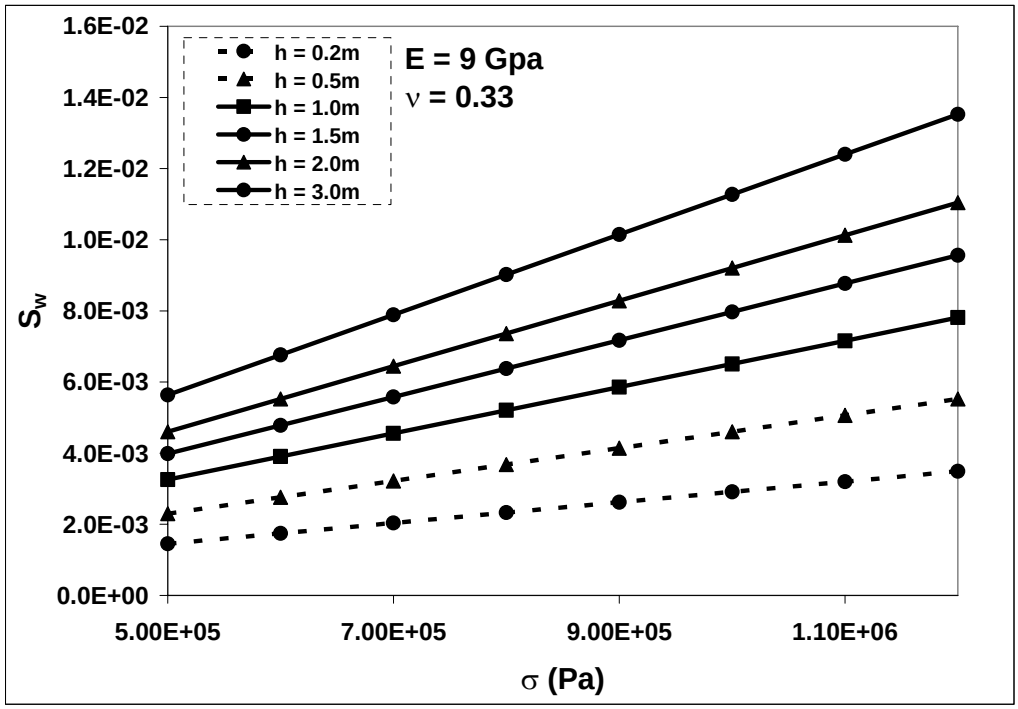

Figure 7 : Sensitivity of the water surface slope to the flexural strength

The above figure shows that in the suggested range of the flexural strength (0.5 MPa to 1.2 MPa), for a given ice thickness, the critical surface stay in the same order of magnitude. The effect of the flexural stress seems to increase with increasing ice thickness. Commonly, 0.5 to 0.6 MPa is used for the value of the flexural stress. In this close range the critical increase in water slope is around 5.10^{-3}.

3.6.2. Elastic modulus

The ice elastic modulus depends on several factors, including temperature, density, ice type, purity, time or frequency of stress, direction of load application, stress history and grain size. As a result, estimates of the elastic modulus can range widely, and values estimated or measured in the field for the elastic modulus of intact freshwater ice range from about 0.4 to 9.8 GPa (Ashton, 1986). The elastic modulus of ice grown in large laboratory tanks ranges from about 4.3 to 8.3 GPa, whereas the elastic modulus of small laboratory specimens is typically higher (USACE, 1999). To investigate the sensitivity of the water slope criteria to the elastic modulus, values of the elastic modulus between 0.4 GPa and 10 GPa were used to reflect the above measured or calculated values. Ice cover thicknesses ranging from 0.2 to 2 m where used. The flexural strength was set to 0.7 MPa and the Poisson's ratio to 0.33. Figure 8 depicts the variation of the water surface slope as a function of the elastic modulus.

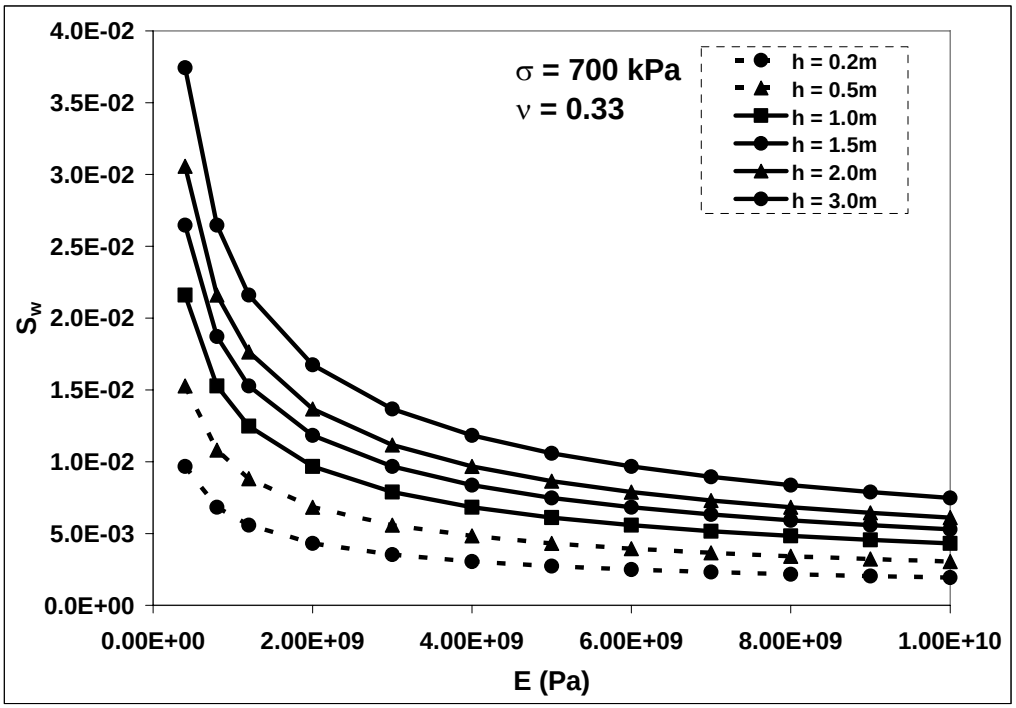

Figure 8 : Sensitivity of the critical water surface slope to the elastic modulus

The above figure shows that the critical water surface slope is very sensitive to low values of the elastic modulus ($E < 3$ GPa). Values of the elastic modulus higher than 3 GPa have less effect on the breaking slope. Most authors consider values of E between 6 GPa (e.g. Billfalk, 1982) and 7 GPa (e.g. Beltaos,2004). In this range, the critical water slope is somewhat insensitive to the variation of E.

3.7. Effect of the wave amplitude

Equation [16] indicates that the water surface slope (S_w) inversely proportional to the wave height (ΔH_{max}). In this section, the effect of the wave height on the critical slope is examined. An ice cover having a flexural strength of 0.7 MPa and an elastic modulus of 9 GPa was considered. Ice thicknesses ranging from 0.2 to 3 m were modeled (Figure 9).

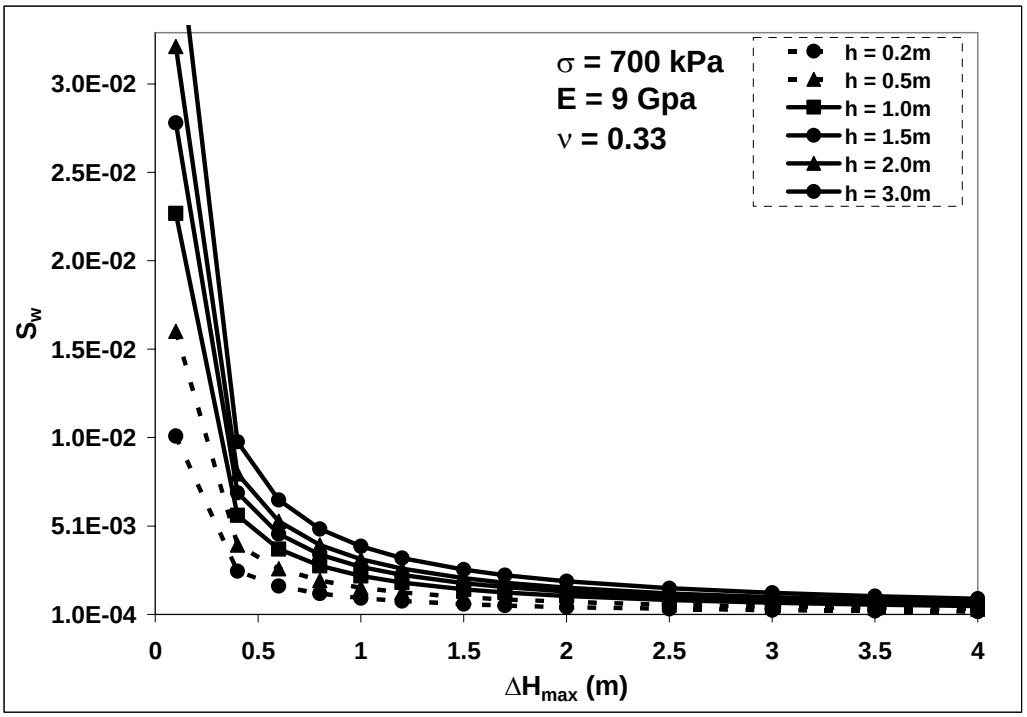

Figure 9 : Variation of the water surface slope as a function of the wave height

The above figure shows that the critical change in water surface slope decreases with increasing wave height. What Figure 9 indicates is that, for given ice properties, there is a critical water surface slope that can cause the ice cover to break. This critical water slope decreases if the incoming wave amplitude increases. Above a wave height of about 1.5 m, the surface slope is no longer a determining factor in breaking the ice cover. The water level change is then too high to break the ice by itself. When the wave height is less 1.5 m, the effect of the slope then starts increasing. Below this range, not only is the change in water level important but the rate at which this change occurs is also a determining factor in inducing stresses in the ice cover. This is interesting conclusion since it is exactly what is expected in the field. The values of the water slope predicted by equation [16] are comparable to field and previous theoretical analysis. Moreover, this equation points out the importance of the combine effects of the change and the rate of change of water level.

It is expected in nature that the water shear as well as the bank resistance would have some effect on the stress induction and crack formation, but these effects are not account for at this point of the study.

4. 2-D analysis

4.1. Introduction

In the previous section, the bank resistance effects where neglected and the ice cover was assumed to be detached from the banks and floating freely on the surface of water. This is not always the case, especially when the river is shallow or the water level increase is moderate. Figure 10 shows a picture of a sheet breaking front observed on the Yukon River by Jasek (2003). The cracking patterns on this picture are far from being transverse. This suggests many hypotheses that should be investigated to have a better understanding of the phenomenon. The bank resistance effects, the non-uniformity of the ice properties (thickness, resistance) are examples of parameters that need to be investigated. The aim of carrying out a 2D analysis is to include more phenomenon into the process of ice rupture in order to evaluate the 1D approach results. This 2D analysis will be based on the theory of plates on elastic foundation (Timoshenko, 1959).

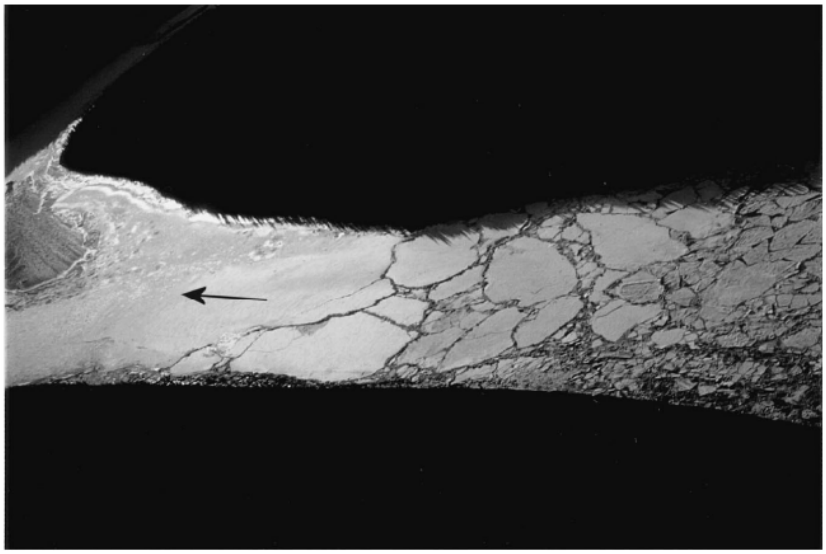

Figure 10 : Observed breakup front on Yukon River. (Jasek, 2003)

The differential equation for the deflection of a plate on an elastic foundation, subjected to a uniform load given by:

$$\frac{\partial^4 y}{\partial x_1^4} + 2\frac{\partial^4 y}{\partial x_1^2 \partial x_2^2} + \frac{\partial^4 y}{\partial x_2^4} = \frac{q}{D} - \frac{ky}{D} \qquad \textbf{[17]}$$

In which y is the deflexion of the plate, x_1 and x_2 the special coordinates; q the applied load; k the foundation modulus and D the flexural rigidity of the plate given by:

$$D = \frac{Eh^3}{12\left(1-\nu^2\right)} \qquad \textbf{[18]}$$

Analytical solutions of equation [17] are given by the author for simple plate configurations and boundary conditions. For more complicated cases, approximate solutions can only be found using numerical tools. In the frame of this study a finite element tool called ANSYS was used. The ANSYS package includes pre-processing, solid modeling, analysis, post-processing, graphics, and design optimization. Details on the software can be found on the ANSYS Inc. website (http://www.ansys.com/products/default.asp).

The technique adopted in ANSYS to model the elastic foundation was simply adding springs elements under the ice cover at each node of the model domain. The apparent Young's modulus (E_s) of the spring was set to:

$$E_s = \frac{\gamma l_s A_o}{A_s} \qquad \textbf{[19]}$$

With l_s and A_s being respectively the length and the area of the spring, A_o is the total area affected to each spring, taken on all elements around the node where the spring is attached (Figure 11).

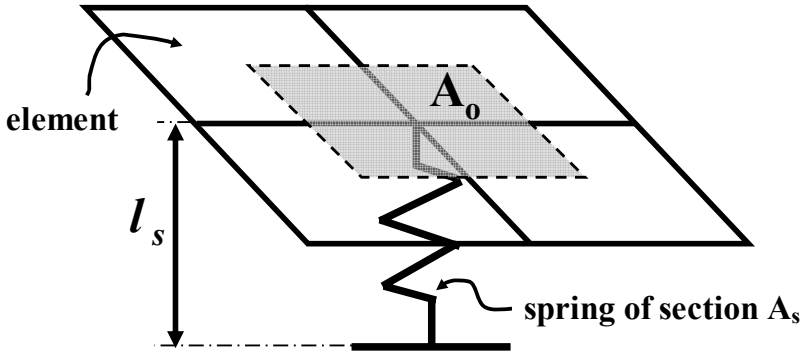

Figure 11 : Connexion of a spring to a node showing the area affected to the spring.

4.2. Analysis of the banks effects

Typically three boundary conditions are applied to the model; a free end upstream, a fixed end downstream and a combination of hinged and fixed end on the banks. The reason for combining two boundary conditions at the banks is the actual model doesn't account for the ice failure itself. Only the elastic behaviour is modeled and therefore, stress will keep developing in the ice even if it exceeds the maximum permitted stress. The technique used to describe the boundary condition at river banks is presented on Figure 12. At each bank, a fictitious extension with a given thickness (h_f) is added to the ice model domain. One edge of the domain extension is fixed and the other hinged. If the thickness of this domain extension is very small, the ice cover will behave as if it was hinged at the bank and the will be no stress concentration at the bank. As the thickness (h_f) of the extension increases, the ice looks more and more like if it was fixed at the banks.

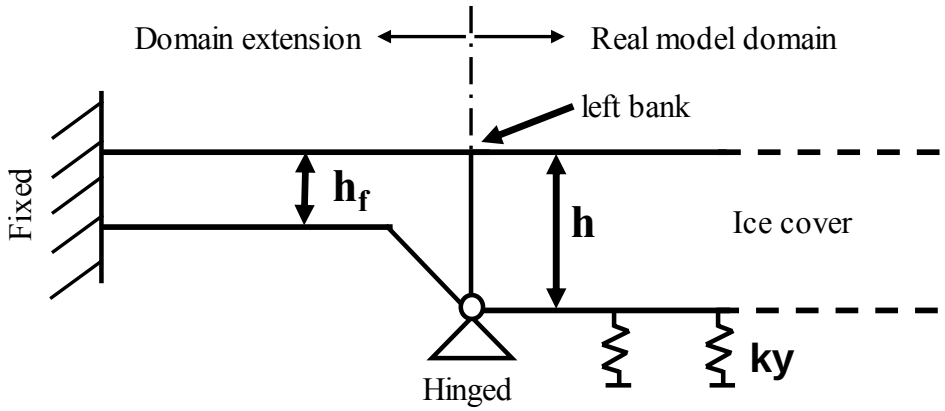

Figure 12 : Technique for modeling banks effect

Figure 13, shows the result of the above described boundary condition modeling approach. In both cases, the ice cover is h = 1 m, E = 6 GPa and ν = 0.33. The change in water level is ΔH_{max} = 0.3 m and a perfectly steep water front has advanced by 75 m into the ice cover. The thickness h_f of the fictitious domain extension is set to 0.025 m and 2 m respectively for the first and the second plots. As expected, for h_f = 2 m, the ice behaves like if it was fixed at the banks and the peak stresses are concentrated along the banks.

For h_f = 0.025 m there is almost no stress concentration at the banks. Instead, the peak stresses are about 30 m from the banks. Which suggest that if the ice was to crack as a result of the water level change, it would crack longitudinally, in a symmetrical way on both sides. This confirms Beltaos (1990) analysis that suggested that wide ice covers with hinged ends would crack at a distance of about 1/5 of the width or less.

For h_f = 0.025 m, it is interesting to compare this 2D numerical solution to the 1D analytical solution presented earlier. Keeping water wave and ice properties described previously unchanged, the stresses induced in the ice cover were computed using 2D model. The results are plotted on Figure 14 as longitudinal profiles of shear bending stresses. Two profiles are plotted for the 2D case, respectively for sections A-A and B-B as shown of Figure 13. The flexural shear stress profile from the 1D analysis looks very similar to the 2D profile from section A-A and the peak values are 0.64 and 0.65 MPa respectively. Nearer the bank at section B-B, the shear bending stress profile changes and the peak stress increase to almost 0.82 MPa. In this case, the peak stress occurs closer to the free edge of the ice cover. These results suggest that by neglecting the bank resistance effects, we are underestimating the peak stresses by around 20%. Moreover, since the peak stresses occur closer to the edge of the ice cover, the cracks would be less spaced than what was suggested by the 1D model. Nevertheless, more investigations need to be conducted before definitive conclusions can be drawn. For instance, the boundary condition approach needs to be improved in other to account for cases where the ice separates from the bank at a point in time. With the current version of the ANSYS model, the boundary condition can't be changed while a solution is being processed.

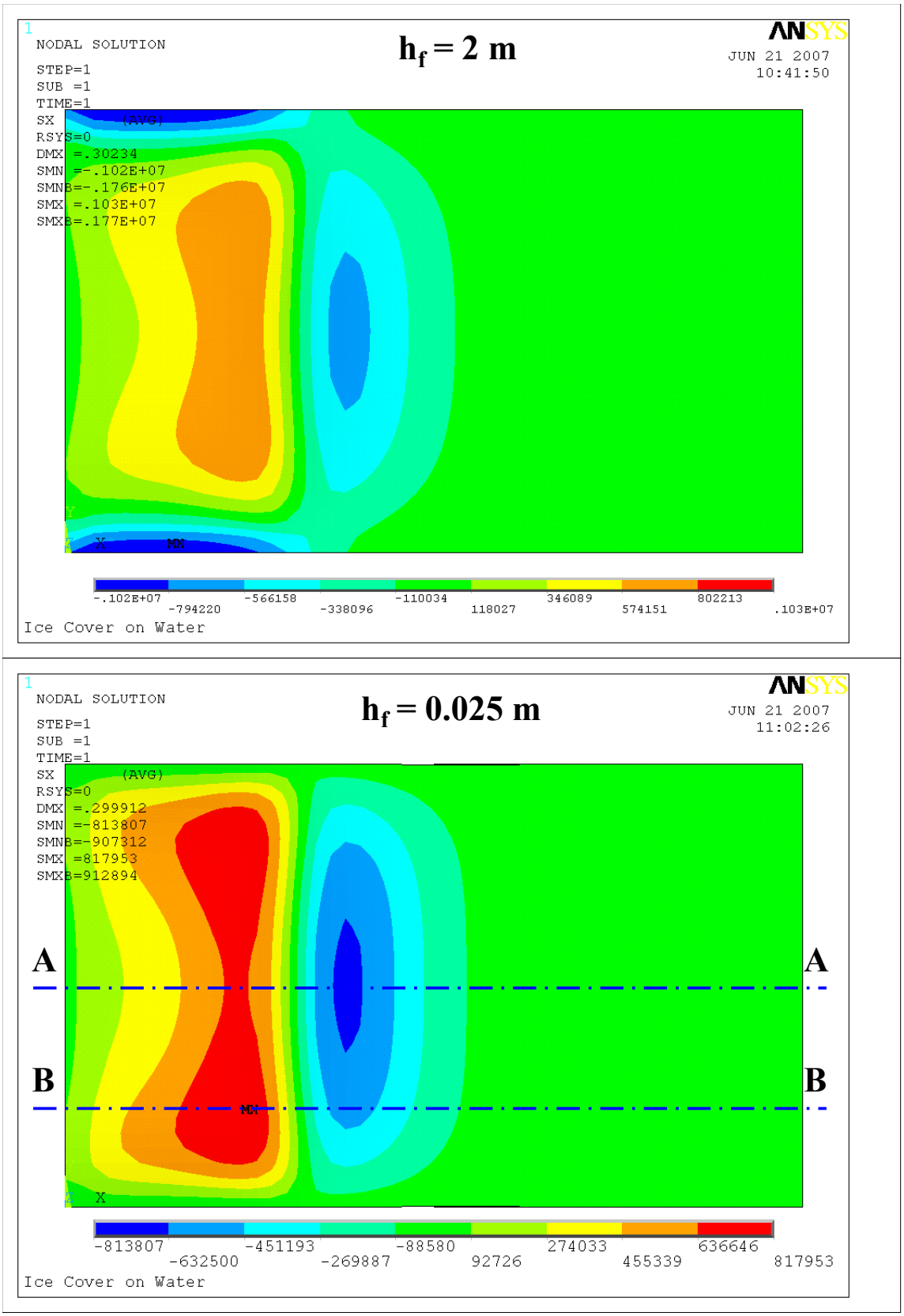

Figure 13 : Model result for bank modeling approach

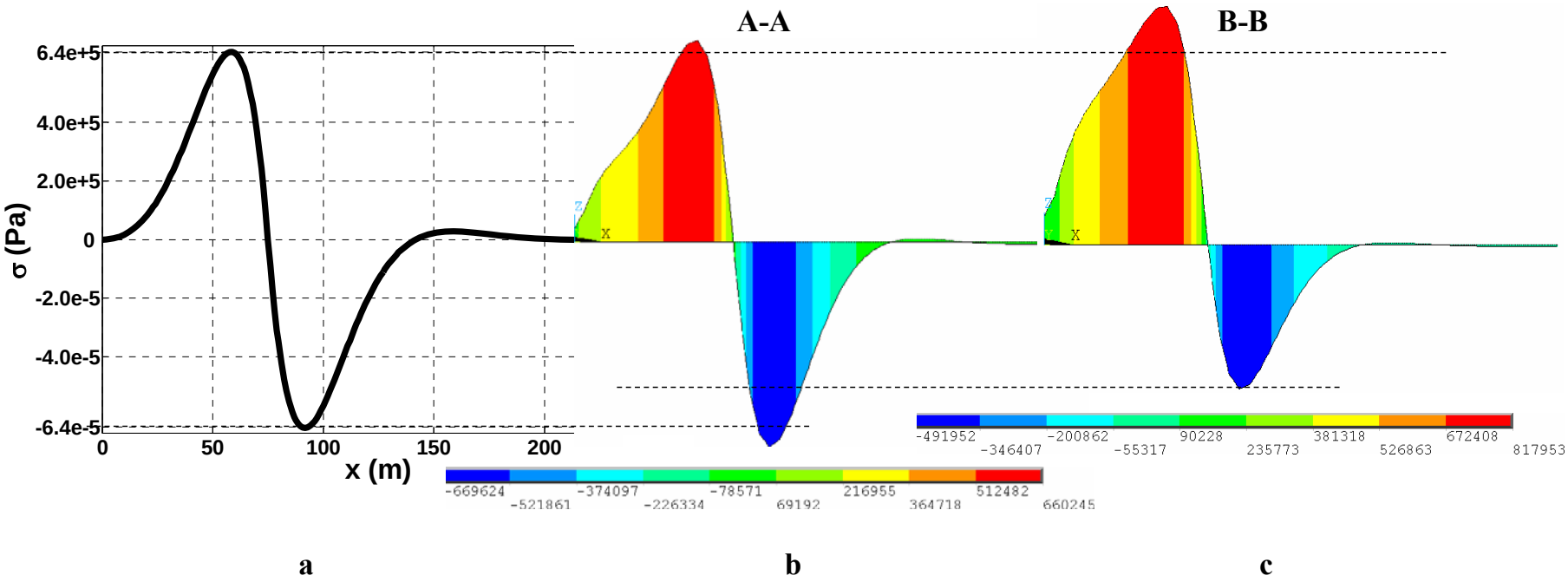

a b c

Figure 14 : Stresses induced in the ice cover: a) 1D model and b), c) 2D model computations

5. Conclusion

In the frame of this study, both 1D and 2D analysis of ice cover bending under distributed loads were presented. Inertia effects where neglected and only buoyancy forces were considered.

The 1D analysis leads to the derivation of a critical increase in water surface slope (S_w) accounting both the ice properties and wave height (equation [16]). The computed critical increases in slope seem to be comparable to field observations during breakup and to previous theoretical results. The results obtain also suggest that the critical increase in water slope decreases if the incoming wave height increases. Above a wave height of about 1.5 m, the increase in surface slope is no longer a determining factor in breaking the ice cover. The water level change is then too high to break the ice by itself. When the wave height is less than about 1 m, the effect of the slope then starts increasing. Below this range, not only is the change in water level important but the rate at which this change occurs is also a determining factor in inducing stresses in the ice cover. This is interesting conclusion since it is exactly what is expected in nature.

At this point in the 2D analysis, a modeling technique to minimize stress concentration at the bank was proposed and works quite well. The results obtained indicated that by neglecting the bank effects, 1D model underestimates the peak stresses by about 20% and overestimate the crack spacing.

6. Future Research

Future work can be summarized in four main points:

- The 2D model results obtained so far are very promising. However, the 2-D model needs to be improved to include the formation of cracks in the ice as critical stress values are exceeded.
- Secondly, once the ice cover criterion is conclusively established, it must then be implemented in hydrodynamic simulations of the breakup event. The main challenge will be the estimation of water surface slope. In fact, due to computation cost, the grid size is often in the range of hundreds of meters to tens of kilometers whereas breaking is a local process and information on the local increase in water surface will be required.
- Thirdly, the proposed criteria must be tested against field and experimental data. The process of data collection is on the way.
- Finally, the effect of the water shear stress on ice cover breakup has not been taken into consideration. We intend to evaluate it experimentally.

Acknowledgments

Funding for this study was provided by the Natural Sciences and Engineering Research Council of Canada (NSERC) through the Unified River Ice Breakup Model project (URIBM). This support is gratefully acknowledged. The authors would also like to thank Hydro Québec for their collaboration in the project.

References

Ashton, G. D. (1986). *River and lake ice engineering*, Water Resources Publications, Littleton, Colo., U.S.A.

Beltaos, S. (1990). "Fracture and Breakup of River Ice Cover." *Canadian Journal of Civil Engineering*, 17(2), 173-183.

Beltaos, S. (2004). "Wave-generated fractures in river ice covers." *Cold Regions Science and Technology*, 40(3), 179-191.

Billfalk, L. (1982). "Breakup of Solid Ice Covers due to Rapid Water Level Variations." *CRREL Report (US Army Cold Regions Research and Engineering Laboratory)*, 24.

Butyagin, I. P. (1972). "Strength of ice and ice cover (nature research on the rivers of Siberia). , Hanover, NH, USA." *USA CRREL Draft Translation* (327).

Daly, S. F. (1993). "Wave-Propagation in Ice-Covered Channels." *Journal of Hydraulic Engineering-Asce*, 119(8), 895-910.

Daly, S. F. (1995). "Fracture of River Ice Covers by River Waves." *Journal of Cold Regions Engineering*, 9(1), 41-52.

Hetenyi, M. (1946). *Beams on elastic foundation*, Univ Michigan Press, Ann Arbor, Mich, United States.

Jasek, M. (2003). "Ice Jam Release Surges, Ice Runs and Breaking Fronts - Field Measurements, Physical Descriptions and Research Needs." *Canadian Journal of Civil Engineering*, 30(1), 113-127.

Kowalczyk, T., and Hicks, F. (2003) " Observations of Dynamic Ice Jam Release on the Athabasca River at Fort McMurray, AB, ." *Proc. 12th Workshop on River Ice.*, Edmonton, AB., 369-392.

Steffler, P. M., and Hicks, F. E. (1994). "Wave-Propagation in Ice-Covered Channels - Discussion." *Journal of Hydraulic Engineering-Asce*, 120(12), 1478-1479.

Timoshenko, S. (1959). *Theory of plates and shells*, McGraw-Hill., Toronto.

USACE. (1999). "Engineering and Design - Ice Engineering." U.S. Army Corps of Engineers, Washington, DC.

Xia, X., and Shen, H. T. (2002). "Nonlinear interaction of ice cover with shallow water waves in channels." *Journal of Fluid Mechanics* 467, 259-268.